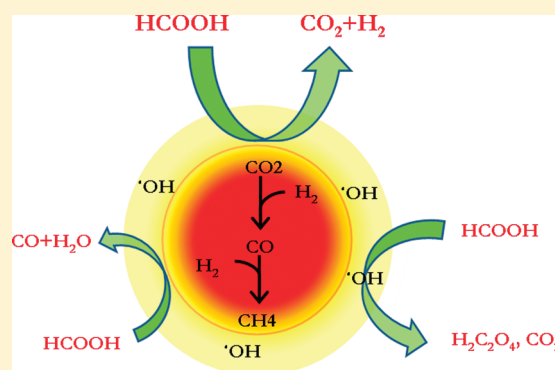


Effect of Ultrasonic Frequency on the Mechanism of Formic Acid Sonolysis

Nathalie M. Navarro,[†] Tony Chave,[‡] Patrick Pochon,[†] Isabelle Bisel,[†] and Sergey I. Nikitenko^{‡,*}[†]CEA/DEN/MAR/DRCP/SCPS/LPCP, CEA Centre de Marcoule, BP 17171, 30207 Bagnols sur Cèze Cedex, France[‡]Institut de Chimie Séparative de Marcoule, UMR 5257 ICSM Site de Marcoule, BP 17171, 30207 Bagnols sur Cèze Cedex, France

Supporting Information

ABSTRACT: The kinetics and mechanism of formic acid sonochemical degradation were studied at ultrasonic frequencies of 20, 200, and 607 kHz under argon atmosphere. Total yield of HCOOH sonochemical degradation increases approximately 6–8-fold when the frequency increased from 20 to 200 or to 607 kHz. At low ultrasonic frequencies, HCOOH degradation has been attributed to oxidation with OH[•] radicals from water sonolysis and to the HCOOH decarboxylation occurring at the cavitation bubble-liquid interface. With high-frequency ultrasound, the sonochemical reaction is also influenced by HCOOH dehydration. Whatever the ultrasonic frequency, the sonolysis of HCOOH yielded H₂ and CO₂ in the gas phase as well as trace amounts of oxalic acid and formaldehyde in the liquid phase. However, CO and CH₄ formations were only detected under high-frequency ultrasound. The most striking difference between low-frequency and high-frequency ultrasound is that the sonolysis of HCOOH at high ultrasonic frequencies initiates Fischer–Tropsch hydrogenation of carbon monoxide.



1. INTRODUCTION

Over the past decade, considerable interest has been expressed in the application of advanced oxidation processes (AOP) to the destruction of hazardous organic compounds in industrial waste streams.¹ Among several different techniques (catalytic wet air oxidation, Fenton process, photocatalytic oxidation, ozonation), sonochemical oxidation is considered to be promising in its degradation of such pollutants.² The ultrasonic irradiation of liquids generates cavitation bubbles, which produce transient heat and highly reactive radical species during their implosive collapse. In aqueous solutions, the homolytic split of H₂O molecules inside the cavitation bubbles leads to the formation of OH[•] radicals, which can react with nonvolatile organic scavengers in the liquid reaction zone surrounding the bubbles.^{3,4} Thus, each cavitation bubble can be considered as a microreactor able to destroy pollutants either by radical reactions or by pyrolysis in bulk at ambient temperature and pressure.

Sonochemical activity depends on several parameters including the liquid's properties (vapor pressure, viscosity, etc.), gas atmosphere, temperature of sonicated solutions, and ultrasonic intensity, and frequency.³ The latter parameter seems to be important in the optimization of the sonochemical processes both with volatile and nonvolatile reagents.⁵ However, the influence of ultrasonic frequency on sonochemical processes is as yet poorly understood. Published results have indicated that ultrasonic irradiation at high frequency enhanced the reaction kinetics

compared to low-frequency ultrasound. For example, in pure water saturated with argon, Pétrier et al. showed that hydrogen peroxide formation was faster at 514 kHz than at 20 kHz.⁶ Hua et al. found that the sonolytic production of hydrogen peroxide in water was about 20-fold higher at 513 kHz than that at 20 kHz in the presence of argon.⁷ Furthermore, it was reported that the formation rate of hydrogen peroxide reached its maximum between 200 and 300 kHz.^{8–10} The frequency's effect on the organic compound degradation rate in aqueous solutions was found to be more complicated and seemed to depend on the physical properties of the molecules involved. For hydrophilic nonvolatile compounds like phenol, the degradation rate is higher at high frequency^{11–13} and reaches a maximum at 200 kHz,^{14,15} whereas for hydrophobic volatile molecules like CCl₄, the reaction rates in general increase with ultrasonic frequency.¹⁴ However, controversial results were found by Hung et al. who reported an optimum frequency at 618 kHz for the sonolytic degradation of CCl₄.¹⁶ Finally, the degradation rate of hydrophilic volatile solutes like 1,4-dioxane increases up to 358 kHz, and then decreases with higher ultrasonic frequencies.¹⁷

Herein, we present a study of the effect of ultrasonic frequency on formic acid sonolysis in aqueous solutions. Formic acid is a

Received: October 1, 2010

Revised: January 20, 2011

Published: February 14, 2011

typical reaction intermediate in various AOP processes¹⁸ and it is therefore important in understanding the mechanism of HCOOH sonochemical degradation. This reaction has been studied by several authors. Henglein et al. showed that at 300 kHz ultrasound, CO, CO₂, and H₂ were the major sonolysis products and only small amounts of oxalic acid were identified in sonicated solutions of concentrated HCOOH.¹⁹ Haissinsky et al. found that in diluted HCOOH solutions sonolytical formation of CO was favored at pH < 2.²⁰ More recently, Gogate et al. reported that the total rate of HCOOH sonolysis is higher at 590 kHz compared to that at 20–50 kHz.^{18,21} However, the detailed analysis of the sonolytical products at different frequencies was not performed. In this work, the sonochemical degradation of HCOOH was studied at 20, 200, and 607 kHz ultrasonic frequencies with other operating parameters (temperature, gas, etc.) strictly controlled. Furthermore, to elucidate the mechanism of HCOOH sonolysis, gaseous, and water-soluble products were analyzed under equivalent reactor conditions. We demonstrated for the first time that an increase in ultrasonic frequency causes not only a change in the total reaction rate but also leads to a modification in the HCOOH sonolysis mechanism.

2. EXPERIMENTAL METHODS

2.1. Materials. Formic acid (98%), hydrogen peroxide (30%), and other analytical grade chemicals were purchased from Aldrich and used without further purification. Deionized water (Milli-Q 18.2 MΩ cm) was used to prepare all aqueous solutions. Argon at 99.999% purity was provided by Air Liquide.

2.2. Reactor Setup and Procedure. Two kinds of ultrasonic equipment were used in this study. The experiments at 20 kHz were performed in a thermostatically controlled closed batch reactor containing 50 mL of solution, and equipped with a 1 cm² irradiating surface area titanium probe and piezoelectric transducer powered by a 20 kHz generator (750 W Sonics). The probe was immersed reproducibly below the surface of the sonicated solution.

The high-frequency reactor consisted of a thermostatted batch reactor equipped with a piezoelectric transducer providing 200 kHz or 607 kHz ultrasound. The transducer was fitted at the bottom of the reactor and connected to a generator with a maximum electrical power of 125W (ELAC Nautik). The volume of sonicated solution was 250 mL. Images of both reactors used in this work are given in Supporting Information.

For all experiments, the solutions were sparged with argon about 1 h before sonication and during the ultrasonic treatment at a controlled rate of 90 mL min⁻¹. The temperature in the reactor during sonolysis was maintained at 20 °C with a Huber Unistat Tango thermo-cryostat and measured by a thermocouple immersed approximately 3 cm below the surface of solution. The acoustic power density, P_{ac} (W mL⁻¹), transmitted to the solution, was measured using a conventional thermal probe method.³ The calibration procedure details are presented in the Supporting Information. The P_{ac} values at 20, 200, and 607 kHz were set at 0.40, 0.18, and 0.26 W mL⁻¹ respectively. To compare the efficiency of the sonochemical processes at different frequencies, the sonochemical yields of the products (G , μmol kJ⁻¹) were applied instead of widely used sonochemical reaction rates (R , M min⁻¹) because G values are independent from the volume of treated solutions and P_{ac} .

2.3. Gas Phase Analysis. Gaseous products of sonolysis were identified using a quadrupole mass spectrometer (PROLAB 300,

Thermo Fisher). The multiple ion monitoring (MIM) mode was employed to follow the evolution of H₂, CO₂, CO, and CH₄ during sonolysis. The yields of H₂, CO₂, and CO were determined after mass spectrometric data calibration with standard H₂/Ar, CO₂/Ar, and CO/Ar gas mixtures (Messer). The statistical error for $G(\text{H}_2)$ and $G(\text{CO}_2)$ values was estimated to be 10%. The accuracy of $G(\text{CO})$ measurements was somewhat lower (~20%) because of higher background signal from N₂ admixtures. Water vapor in the outlet gas was trapped with molecular sieves (Aldrich, 3 Å) prior the mass spectrometric analysis. The emission of CO, CO₂, and CH₄ during sonolysis was confirmed qualitatively using gaseous IR-spectroscopy (Nicolet Magna-IRTM Spectrometer, model 750).

2.4. Liquid Phase Analysis. Water-soluble sonolysis products were analyzed with HPLC using a DIONEX Ultimate 3000 instrument. Carboxylic acids in sonicated solutions were separated on a METACARB 67H column (Varian) pre-equilibrated at 35 °C. The mobile phase was an 0.01 N H₂SO₄ solution (0.8 mL min⁻¹). Carboxylic acids were then measured using a UV detector at 210 nm.

Formaldehyde was determined by DNPH (2,4-dinitrophenylhydrazine) derivatization followed by HPLC analysis with a C18 column (Dionex) at 30 °C. The mobile phase was a mixture of 50% water and 50% acetonitrile (1 mL min⁻¹). Analysis was performed with UV detector at 360 nm. The formaldehyde concentrations were estimated after a data calibration with different solutions prepared using a commercial formaldehyde solution (Aldrich, 36%) (Supporting Information).

Hydrogen peroxide was monitored by spectrophotometry with Ti(IV) in 1 M HNO₃ ($\lambda = 411$ nm, $\epsilon = 707$ cm⁻¹ M⁻¹).²² The statistical error for H₂O₂ formation rate was estimated to be 10%.

3. RESULTS AND DISCUSSION

3.1. Water Sonolysis. The kinetics of H₂ and H₂O₂ formation during pure water sonolysis at selected ultrasonic frequencies was studied during the first stage of work. Formation of both products follows zero order kinetics at all studied ultrasonic frequencies. It is generally recognized that in argon atmosphere H₂ and H₂O₂ are formed due to the homolytical split of water molecules inside the cavitation bubbles, followed by the mutual recombination of H• and OH• species inside the bubble (H• + H•) and at the bubble-liquid (OH• + OH•) interface:³



Table 1 shows the yields of H₂ and H₂O₂ during water sonolysis obtained at different ultrasonic frequencies. These results confirm published data⁶ that $G(\text{H}_2\text{O}_2)$ is greater under high-frequency ultrasound than at low frequencies. For example, Table 1 demonstrates that at 607 kHz the $G(\text{H}_2\text{O}_2)$ value is almost seven times higher than that obtained at 20 kHz. Surprisingly, the observed $G(\text{H}_2\text{O}_2)$ at 20 kHz is lower than that of H₂ obtained at the same conditions. To the best of our knowledge, this is the first observation of such a phenomenon. In contrast, at high-frequency ultrasounds the yields of both

Table 1. Effect of Ultrasonic Frequency on G Values for H₂O₂ and H₂ during Water Sonolysis under Argon at 20 °C, $\sigma = \pm 10\%$

frequency (kHz)	G ($\mu\text{mol kJ}^{-1}$)	
	H ₂ O ₂	H ₂
20	0.06	0.12
20 ^a	0.05	-
200	0.28	0.28
514 ^a	0.23	-
607	0.46	0.49

^a Ref 6; 24 °C, Ar.

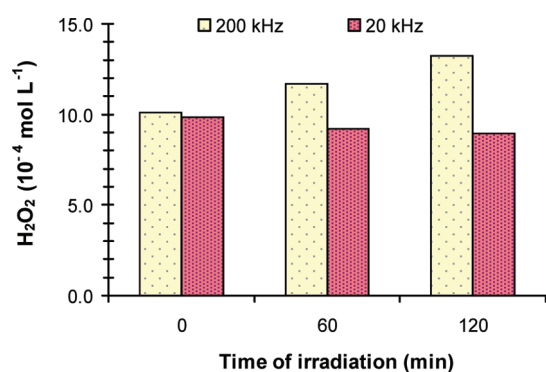


Figure 1. Effect of ultrasonic frequency (20 and 200 kHz) on the sonolysis of H₂O₂ mol L⁻¹ under argon, 20 °C.

products are fairly similar, which fits well with the reaction scheme (1–3). It has been suggested that H₂O₂ can be degraded at low ultrasonic frequency. To verify this hypothesis, we performed experiments on the sonolysis of 10⁻³ M H₂O₂ aqueous solutions at 20 and 200 kHz in the presence of argon.

Figure 1 clearly shows a difference in H₂O₂ behavior between 20 and 200 kHz ultrasound. During sonication at 20 kHz, the concentration of H₂O₂ decreases, whereas at 200 kHz an increase in H₂O₂ concentration can be observed. The degradation of H₂O₂ at low-frequency ultrasound is most probably related to its catalytic decomposition on titanium particles coming from the cavitation erosion of the titanium probe. A control experiment under mechanical stirring in the presence of titanium powder (Supporting Information) showed relatively rapid H₂O₂ decomposition, confirming this hypothesis. The cavitation erosion is known to be much stronger at low ultrasonic frequency compared to high-frequency ultrasound.^{23,24} Therefore, the catalytic decomposition of H₂O₂ would be expected to be more effective at 20 kHz than under high-frequency ultrasound.

3.2. HCOOH Sonolysis. Table 2 shows the G(H₂O₂) values as a function of HCOOH concentration at the ultrasonic frequencies studied. It can be seen that whatever the ultrasonic frequency, the yield of hydrogen peroxide decreases with increasing HCOOH concentration, indicating effective scavenging of OH[•] radicals:



Table 2. Yield of H₂O₂ ($\mu\text{mol kJ}^{-1}$) during Formic Acid Sonolysis in Argon at 20 °C

frequency (kHz)	water	HCOOH (mol L ⁻¹)		
		0.1	1.0	3.0
20	0.06	0.06	0.02	0.01
200	0.28	0.17	0.07	0.04
607	0.46	0.32	0.15	0.05

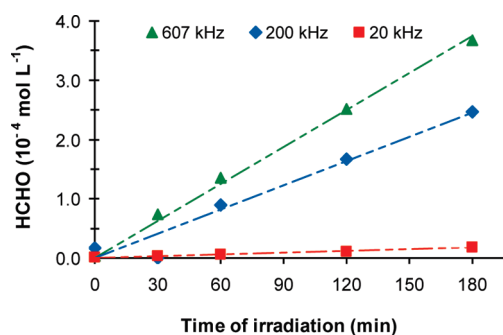


Figure 2. Evolution of HCHO concentration with sonication time during HCOOH sonolysis [HCOOH] = 3M, 20 °C, Ar; $P_{ac} = 0.40 \text{ W mL}^{-1}$, 0.18 W mL^{-1} and 0.26 W mL^{-1} for 20, 200, and 607 kHz, respectively.

The reactions 4 and 5 can be summarized as:



From reaction 6 it follows that, for the radical mechanism, G(CO₂) should not be higher than G(H₂O₂) in pure water.

In the liquid phase, small amounts ($\sim 10^{-5}$ to 10^{-4} mol L⁻¹ after 3 h of sonolysis) of oxalic acid were identified at all ultrasonic frequencies and for all concentrations of formic acid, which is in agreement with Henglein's work.¹⁹ It is likely that H₂C₂O₄ is formed due to the HCOO[•] radical recombination at the bubble liquid interface:¹⁹



Surprisingly, formaldehyde was also detected in the sonicated HCOOH solutions. A clear signal was detected by means of HPLC with UV detector at 360 nm after sonicated sample pretreatment with DNPH. Figure 2 shows the linear increase of HCHO concentration with sonication time. After 3 h of sonolysis at high frequency, the HCHO concentration reached approximately $(2.5\text{--}3.7) \times 10^{-4}$ mol L⁻¹, whereas at 20 kHz its concentration was at least 10 times lower. To the best of our knowledge, this is the first observation of HCHO formation during sonolysis of carboxylic acid solutions. A probable mechanism for its formation will be discussed later.

The mass spectrometric analysis of the outlet gas revealed the formation of CO, CO₂, and H₂ as the principal gaseous products of HCOOH sonolysis (Figure 3), in agreement with previously published data.^{19,20} Figure 3 clearly shows a more rapid HCOOH sonolysis under high-frequency ultrasound compared to that at 20 kHz.

The G(CO₂) values increased with ultrasonic frequency and HCOOH concentration. In diluted HCOOH (0.1 M), the yield of H₂O₂ was comparable with the value obtained during pure water sonolysis, indicating that the formation of CO₂ via radical

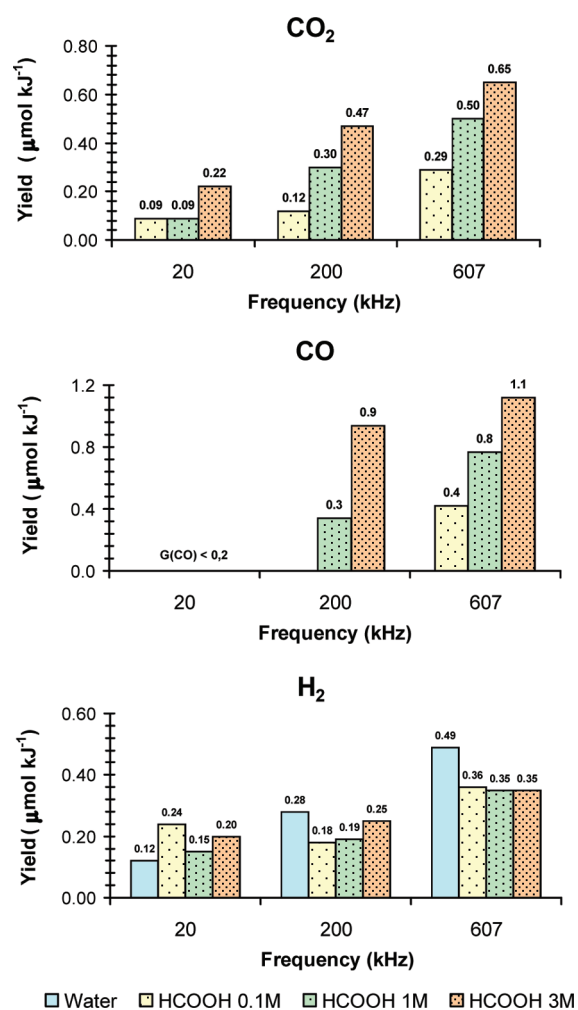


Figure 3. Yields of H₂, CO₂, and CO during HCOOH sonolysis at 20, 200, and 607 kHz under argon atmosphere, 20 °C.

reaction with hydroxyl radical (reaction 5) is insignificant. The formation of CO₂ can be explained by HCOOH decarboxylation:

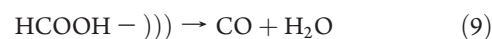


In 1–3 M HCOOH, the yield of H₂O₂ decreases, and the contribution of radical reactions becomes more important. However, in contrast to eq 6, the G(CO₂) values are higher than G(H₂O₂) obtained during pure water sonolysis, indicating that degradation by radical reactions and by HCOOH decarboxylation occurred simultaneously.

Partial vapor pressure of HCOOH in relatively diluted aqueous solutions (0.1–3.0 M) is known to be lower than that of water at room temperature.^{25,26} Consequently, the gas phase of the cavitation bubble would be depleted on HCOOH molecules under our conditions, and reaction 8 should occur preferably in the liquid reaction zone surrounding the cavitation bubble. The temperature at the interface is indeed high enough to consider a hydrothermal decomposition of formic acid in this region.⁴ It is well known that there are two reaction channels in the thermal decomposition of formic acid: HCOOH decarboxylation (reaction 8) and the dehydration reaction that produces carbon monoxide:

Table 3. Total Yield of HCOOH Sonolysis $G(\text{HCOOH}) = G(\text{CO}) + G(\text{CO}_2)$ and the Yield Ratio $G(\text{CO})/G(\text{CO}_2)$ as a Function of Ultrasonic Frequency and HCOOH Concentration; Ar, 20 °C, $\sigma = \pm 30\%$

frequency (kHz)	[HCOOH] (mol L ⁻¹)	G(HCOOH) (μmol kJ ⁻¹)	G(CO) / G(CO ₂)
20	0.1	0.1	below the quantification limit
	1	0.1	
	3	0.2	
200	0.1	0.1	
	1	0.6	1.1
	3	1.4	2.0
607	0.1	0.7	1.5
	1	1.3	1.5
	3	1.8	1.7



The yield of CO is extremely sensitive to ultrasonic frequency. For 20 kHz, figure 3 reveals an amount of CO in the outlet gases below the detection limits in all the HCOOH concentrations studied. At 200 kHz, the formation of CO was always observed except in 0.1 M HCOOH solution. For more concentrated solutions, the yield of CO is comparable to that of CO₂ and increased with the HCOOH concentration. At 607 kHz, the formation of CO was observed for all HCOOH concentrations. The G(CO) values increased with the HCOOH concentration, similarly to observations at 200 kHz.

Table 3 demonstrates that under high-frequency ultrasound, the ratio of the sonochemical yields of CO and CO₂ increased with HCOOH concentration from ~1.1 (1 M HCOOH) to ~2.0 (3.0 M HCOOH). This ratio is much less than that reported for gas-phase HCOOH thermolysis ([CO]/[CO₂] ~10).²⁷ Therefore, the G(CO)/G(CO₂) ratio observed in our experiments confirms the assumption that HCOOH sonolysis occurs in the liquid reaction zone rather than in the gas phase of the cavitation bubble. Several studies have shown that H₂O molecules catalyze HCOOH decarboxylation under hydrothermal conditions, providing a higher yield of CO₂ compared to that of CO.^{28–30} Thus, presuming HCOOH sonochemical degradation in the liquid phase, the G(CO)/G(CO₂) ratio should be smaller than 1. However, Table 3 indicates a clearly higher yield for CO observed in sonochemical experiments. Furthermore, the relatively high influence of the decarboxylation reaction pathway in HCOOH sonochemical degradation as well as H₂ formation during water sonolysis supposes observed G(H₂) values higher than G(H₂) values obtained during pure water sonolysis. This is true for low-frequency ultrasound (Figure 3). However, Figure 3 also shows that under high-frequency ultrasound the G(H₂) value is lower than that in pure water for all concentrations of HCOOH. These contradictions between observed and expected reaction yields can be understood considering the secondary gas phase sonochemical processes initiated under high-frequency ultrasound. It has been reported that CO₂ can be reduced sonochemically to CO in water due to the reaction with H₂ coming from sonochemical water split:^{31,32}



In our system, H₂ from water sonolysis and decarboxylation

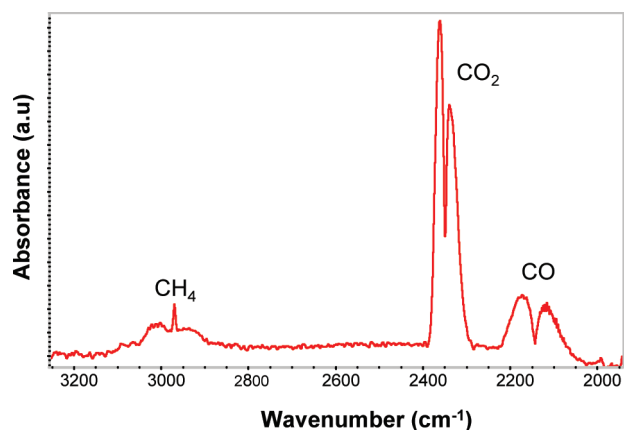


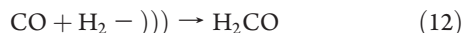
Figure 4. IR-spectrum of the outlet gas obtained after 1 h of 3 M HCOOH sonolysis, 20 °C, 200 kHz, argon.

reaction 8 reacted with CO₂ formed after the radical oxidation (4–5) and decarboxylation (8) of HCOOH. Note here that CO₂ is more soluble in water than Ar and thus can accumulate in the reaction medium.³² At 20 kHz ultrasound, the amount of CO₂ produced is low and, consequently, the amount of CO formed in the secondary processes is also insignificant. At low-frequency ultrasound, the H₂ formed does not participate in any secondary reactions and its yield in HCOOH solutions is higher than in pure water. However, under high-frequency ultrasound the concentration of CO₂ is sufficient to provide significant consumption of H₂.

The mass spectra of the outlet gas at high-frequency sonolysis revealed the appearance of a signal with $m/z = 16$ simultaneously with the CO signal ($m/z = 28$) (Supporting Information). This signal could be assigned to methane formation. Indeed, the FTIR spectra of the outlet gas collected under these conditions (Figure 4) exhibited a peak at 2900 cm⁻¹ typical for C–H stretching vibrations in CH₄ molecules. This result clearly points to methane formation during the sonolysis of HCOOH under high-frequency ultrasound, which is in agreement with the recent finding of Harada who reported the sonochemical reduction of CO₂ to CH₄ in water in the presence of a CO₂–H₂ gas mixture.³³ The FTIR spectra also indicate the presence of CO and CO₂ in the outlet gas. Under our conditions, the formation of CH₄ can be explained by the secondary CO hydrogenation inside the cavitation bubble, similar to the well-known Fischer–Tropsch synthesis:³⁴



This reaction is not observed under low-frequency ultrasound because of the negligibly low yield of CO at all HCOOH concentrations studied. In view of the proposed hydrogenation mechanism, the formation of formaldehyde could be considered as an intermediate stage of CH₄ formation:



Formation of oxygenated impurities during the catalytic hydrogenation of CO has been reported in the presence of large amounts of water vapor.³⁴ It should be noted here that Fischer–Tropsch synthesis under silent conditions needs catalysts. In our experiments, CO hydrogenation occurred due to the extreme local conditions created by acoustic cavitation inside the cavitation bubbles. The absence of hydrocarbons heavier than CH₄

indicates a local temperature much higher than 300 °C during sonochemical hydrogenation of CO, according to thermodynamic data.³⁴

The total yield of HCOOH sonochemical degradation can be expressed as:

$$\begin{aligned} G(\text{HCOOH}) = & G(\text{CO}) + G(\text{CO}_2) + G(\text{CH}_4) \\ & + \frac{1}{2} G(\text{H}_2\text{C}_2\text{O}_4) + G(\text{H}_2\text{CO}) \end{aligned} \quad (13)$$

Presuming $G(\text{CO}) + G(\text{CO}_2) \gg G(\text{CH}_4) + \frac{1}{2} G(\text{H}_2\text{C}_2\text{O}_4) + G(\text{H}_2\text{CO})$, eq 13 can be simplified as: $G(\text{HCOOH}) = G(\text{CO}) + G(\text{CO}_2)$. Table 3 summarizes $G(\text{HCOOH})$ values at different ultrasonic frequencies. Generally speaking, Table 3 reveals that the sonolysis of HCOOH is approximately 6–8 times more effective under high-frequency ultrasound than under 20 kHz ultrasound. Several reasons can be given for such a significant difference. First, the distribution of the cavitation field is different between low- and high-frequency ultrasound.³⁵ A 20 kHz horn system gives a limited conical cavitation zone near the horn tip while high frequencies ($f \geq 200$ kHz) tend to give a more diffuse, widely distributed zone of cavitation. It can be assumed that a much larger number of cavitation bubbles can be generated under high-frequency ultrasound in a treated volume of liquid at any time for the same specific absorbed acoustic power. Consequently, at high frequency a larger volume of solution is directly submitted to ultrasonic irradiation compared to 20 kHz ultrasound. Second, the resonance size of a single cavitation bubble is inversely correlated to the ultrasonic frequency:¹⁷

$$R_r^2 = \frac{3KP_0}{\rho\omega_r^2} \quad (14)$$

where R_r^2 is the resonant bubble radius, $K = C_p/C_v$ is the polytropic index, P_0 is the hydrostatic pressure, ρ is the density of the liquid, and ω_r is the radial resonant frequency. As the frequency increases, the resonant radius of the cavitation bubbles decreases. Smaller bubbles require fewer acoustic cycles before reaching their resonant size. This leads to cavitation events occurring at a faster rate at higher ultrasonic frequency. A decrease in the bubble size causes a significant increase in its surface area to volume ratio, SA/V. For example, the SA/V ratio increases from 0.02 to 0.52 μm^{-1} when the ultrasonic frequency increases from 20 to 607 kHz. In other words, the relative effective volume of the liquid overheated shell for each cavitation bubble rises considerably as frequency increases. Both factors, total volume of the cavitation zone and single bubble SA/V ratio, are very important for the sonochemical reactions occurring at bubble/liquid interface, as in the HCOOH sonolysis studied in this work.

The ultrasonic frequency also could influence the intrabubble conditions. Until recently, it was thought that low-frequency ultrasound primarily generated transient cavitation and high-frequency ultrasound primarily generates stable cavitation. However, recent studies of multibubble sonoluminescence and sonochemistry have revealed the existence of transient cavitation at high ultrasonic frequency.³⁶ Moreover, it has been shown very recently that the increase of ultrasonic frequency causes a population of electronically OH($C^2\Sigma^+$) and vibrationally OH($A^2\Sigma^+$, ν_1) excited radicals during water sonolysis in the presence of noble gases.³⁷ Potentially these species would have advanced oxidizing properties.³⁷ Further studies are required to elucidate the impact of ultrasonic frequency on extreme

conditions created by acoustic bubble collapse and related sonochemical activity.

4. CONCLUSIONS

Ultrasonic frequency is a critical parameter in the sonolysis of formic acid in aqueous solutions. The total yield of 0.1–3.0 M HCOOH sonochemical degradation increases approximately 6- to 8-fold when the frequency increases from 20 kHz to 200 or 607 kHz under argon atmosphere. In agreement with the literature, CO₂, CO, H₂, and oxalic acid are the main products of HCOOH sonolysis. Moreover for the first time, formaldehyde and methane were detected. In a diluted solution (0.1 M HCOOH), sonochemical degradation occurs mostly by HCOOH decarboxylation in the liquid reaction zone at the bubble/solution interface for all ultrasonic frequencies studied. When the HCOOH concentration becomes higher (1.0–3.0 M), degradation also occurs via simultaneous OH[•] radical scavenging. Under high-frequency ultrasound the reaction is also influenced by HCOOH dehydration. The most striking feature of this work is that the high-frequency ultrasonic treatment initiated secondary hydrogenation reactions of CO₂ and CO. Under high ultrasonic frequency CO₂ reacted with H₂ to produce CO. Thereby, at 200 and 607 kHz CO is the major product and the yield of H₂ is even lower than that obtained during pure water sonolysis. Sonochemically driven Fischer–Tropsch hydrogenation of CO led to the formation of methane and formaldehyde as byproduct of HCOOH degradation. Finally, we found catalytic decomposition of sonochemically formed H₂O₂ on the surface of titanium particles formed during cavitation erosion of the ultrasonic probe under low-frequency ultrasound. This finding is important for the proper interpretation of sonochemical experiments.

■ ASSOCIATED CONTENT

S Supporting Information. Additional figures and tables, with a more detailed description of the materials and methods used for the study. This material is available free of charge via the Internet at <http://pubs.acs.org>.

■ AUTHOR INFORMATION

Corresponding Author

*E-mail: serguei.nikitenko@cea.fr. Phone: +33(0) 466 339 251. Fax: +33(0) 466 796 027.

■ ACKNOWLEDGMENT

N. Navarro thanks CEA/DEN/MAR/DRCP/SCPS for financial support of her PhD thesis. The authors are grateful to J.P. Donnarel and D. Sans for their help in HPLC and FTIR analysis.

■ REFERENCES

- (1) Andreozzi, R.; Caprio, V.; Insola, A.; Marotta, R. *Catal. Today* **1999**, *53*, 51–59.
- (2) Adewuyi, Y. G. *Ind. Eng. Chem. Res.* **2001**, *40*, 4681–4715.
- (3) Mason, T. J.; Lorimer, J. P. *Applied Sonochemistry. The Uses of Power Ultrasound in Chemistry and Processing*; Wiley-VCH: Weinheim, 2002.
- (4) Suslick, K. S.; Hammerton, D. A.; Cline, R. E. *J. Am. Chem. Soc.* **1986**, *108*, 5641–5642.
- (5) Petrier, C.; Francony, A. *Ultrasonics Sonochemistry* **1997**, *4*, 295–300.

- (6) Petrier, C.; Jeunet, A.; Luche, J. L.; Reverdy, G. *J. Am. Chem. Soc.* **1992**, *114*, 3148–3150.
- (7) Hua, I.; Hoffmann, M. R. *Environ. Sci. Technol.* **1997**, *31*, 2237–2243.
- (8) Mendez-Arriaga, F.; Torres-Palma, R. A.; Petrier, C.; Esplugas, S.; Gimenez, J.; Pulgarin, C. *Water Res.* **2008**, *42*, 4243–4248.
- (9) Jiang, Y.; Petrier, C.; Waite, T. D. *Ultrasonics Sonochemistry* **2006**, *13*, 415–422.
- (10) Koda, S.; Kimura, T.; Kondo, T.; Mitome, H. *Ultrasonics Sonochemistry* **2003**, *10*, 149–156.
- (11) Petrier, C.; Lamy, M. F.; Francony, A.; Benahcene, A.; David, B.; Renaudin, V.; Gondrexon, N. *J. Phys. Chem.* **1994**, *98* (41), 10514–10520.
- (12) Berlan, J.; Trabelsi, F.; Delmas, H.; Wilhelm, A. M.; Petrigiani, J. F. *Ultrasonics Sonochemistry* **1994**, *1*, S97–S102.
- (13) Chen, J. W.; Chang, J. A.; Smith, G. V. *Chem. Eng. Prog. S. Ser.* **1971**, *67*, 18–26.
- (14) Petrier, C.; Francony, A. *Water Sci. Technol.* **1997**, *35*, 175–180.
- (15) Okouchi, S.; Nojima, O.; Arai, T. *Water Sci. Technol.* **1992**, *26*, 2053–2056.
- (16) Hung, H. M.; R. Hoffmann, M. R. *J. Phys. Chem A* **1999**, *103*, 2734–2739.
- (17) Becket, M. A.; Hua, I. *J. Phys. Chem. A* **2001**, *105*, 3796–3802.
- (18) Gogate, P. R.; Mujumdar, S.; Pandit, A. B. *Adv. Environ. Res.* **2003**, *7*, 283–299.
- (19) Hart, E. J.; Henglein, A. *Radiat. Phys. Chem.* **1988**, *32*, 11–13.
- (20) Haïssinsky, M.; Klein, R. *J. Chim. Phys. Phys. Chim. Biol.* **1968**, *65*, 336–344.
- (21) Gogate, P. R.; Pandit, A. B.; Wilhelm, A. M.; Ratsimba, B.; Delmas, H. *Water Res.* **2006**, *40*, 1697–1705.
- (22) Nikitenko, S. I.; Le Naour, C.; Moisy, P. *Ultrasonics Sonochemistry* **2007**, *14*, 330–336.
- (23) Karimi, A.; Martin, J. L. *Cavitation Erosion of Materials. Int. Met. Rev.* **1986**, *31*, 1–26.
- (24) Fatjo, G. A.; Pérez, A. T.; Hadfield, M. *Ultrasonics Sonochemistry* **2011**, *18*, 73–79.
- (25) Ito, T.; Yoshida, F. *J. Chem. Eng. Data* **1963**, *8*, 315–320.
- (26) Conti, J. J.; Othmer, D. F.; Gilmont, R. J. *Chem. Eng. Data* **1960**, *5*, 301–307.
- (27) Saito, K.; Kakumoto, T.; Kuroda, H.; Torii, S.; Imamura, A. *J. Chem. Phys.* **1984**, *80*, 4989–4994.
- (28) Yu, J.; Savage, P. E. *Ind. Eng. Chem. Res.* **1998**, *37*, 2–10.
- (29) Chen, H. T.; Chang, J. G.; Chen, H. L. *J. Phys. Chem. A* **2008**, *112*, 8093–8099.
- (30) Bjerre, A. B.; Sorensen, E. *Ind. Eng. Chem. Res.* **1992**, *31*, 1574–1577.
- (31) Henglein, A. *Z. Naturforsch.* **1985**, *40b*, 100–107.
- (32) Harada, H. *Ultrasonics Sonochemistry* **1998**, *5*, 73–77.
- (33) Harada, H.; Hosoki, C.; Ishikane, M. *J. Photochem. Photobiol. A* **2003**, *160*, 11–17.
- (34) Anderson, R. B. *The Fischer–Tropsch Synthesis*; Academic Press, Inc.: New York, 1984.
- (35) Price, G. J.; Harris, N. K.; Stewart, A. J. *Ultrasonics Sonochemistry* **2010**, *17*, 30–33.
- (36) Ashokkumar, M.; Lee, J.; Iida, Y.; Yasui, K.; Kozuka, T.; Tuziuti, T.; Towata, A. *Phys. Chem. Chem. Phys.* **2009**, *11*, 10118–10121.
- (37) Pflieger, R.; Brau, H.-P.; Nikitenko, S. I. *Chem.—Eur. J.* **2010**, *16*, 11801–11803.